ture. Substituting these values into eq 23 leads to 262 ns as the time required for a naphthalene molecule to diffuse from the interior of an SDS micelle to the surface. The significant fact is that naphthalene triplet is sufficiently long lived [$\tau_N T \geq (1.14 \pm 0.07) \times 10^{-5}$ s] to diffuse out of the micellar interior and transfer its energy to terbium chloride.

The role of micelles is the simple, albeit vital, compartmentalization of the energy transfer partners. It separates naphthalene molecules from each other obviating thereby triplet-triplet annihilation (reaction 12). Additionally, by binding the terbium chloride electrostatically to the negatively charged micellar surface, the effective concentration of the acceptor molecules is substantially increased. The concentration of countercations in the micellar Stern layer has been estimated to be 3.0 M.[29] In aqueous solution reaction 12 successfully competes with reaction 15 and thus energy transfer is not observable. These results emphasize the important roles artificial and real membranes play in enhancing the efficiency of energy transfer.

Acknowledgment. Support of this work by the National Science Foundation and by the Robert A. Welch Foundation is gratefully acknowledged. It is a pleasure to acknowledge the benefits derived from discussions with Professor R. H. Hedges.

References and Notes

(1) M. Dixon and E. C. Webb, "Enzymes", Longmans, London, 1964.
(2) J. H. Fendler and E. J. Fendler, "Catalysis in Micellar and Macromolecular Systems", Academic Press, New York, N.Y., 1975.
(3) J. H. Fendler, *Acc. Chem. Res.*, **9**, 153 (1976).
(4) H. Ti Tien, *Photochem. Photobiol.*, **24**, 97 (1976).
(5) A. D. Bangham, *Prog. Biophys. Mol. Biol.* **18**, 29–95 (1968).
(6) D. Papahadjopoulos and K. K. Kimelberg, *Prog. Surf. Sci.*, **4**, 141 (1973).
(7) A. D. Bangham, M. W. Hill, and N. G. A. Miller, *Methods Membr. Biol.* **11**, 38 (1974).
(8) E. L. Wehry, "Modern Fluorescence Spectroscopy", Plenum Press, New York, N.Y., 1976.
(9) G. Strauss, *Photochem. Photobiol.*, **24**, 141 (1976).
(10) S. A. Alkaitis, M. Gratzel, and A. Henglein, *Ber. Bunsenges. Phys. Chem.*, **79**, 541 (1975).
(11) S. A. Alkaitis and M. Gratzel, *J. Am. Chem. Soc.*, **98**, 3549 (1976).
(12) A. Heller and E. Wasserman, *J. Chem. Phys.*, **43**, 949 (1965).
(13) K. Shinoda, T. Nakagawa, B. Tamamushi, and T. Isemura, "Colloidal Surfactants", Academic Press, New York, N.Y., 1963.
(14) P. S. Sheih, Dissertation, Texas A&M University, May 1976.
(15) A. Romero, J. Sunamoto, and J. H. Fendler, *Colloid Interface Sci.*, **V**, 111 (1976).
(16) L. A. Shaver and L. J. C. Love, *Appl. Spectrosc.*, **29**, 485 (1965).
(17) I. Isenberg and R. Dyson, *Biophys. J.*, **9**, 1337 (1969).
(18) We are grateful to Dr. Silvio DiGregorio, SPEX Industries, Inc., Metuchen, N.J., for determining the phosphorescence spectra and lifetime using the prototype phosphorescence attachment of the SPEX Fluorolog.
(19) H.-F. Eicke, J. C. W. Shepherd, and A. Steinemann, *J. Colloid Interface Sci.*, **56**, 168 (1976).
(20) R. M. Rosenberg, H. L. Crespi, and J. J. Katz, *Biochim. Biophys. Acta*, **175**, 31 (1969).
(21) R. Foster and C. A. Fyfe, *Prog. Nucl. Magn. Reson. Spectrosc.* **4** (1969).
(22) R. R. Hautala, N. E. Schore, and N. J. Turro, *J. Am. Chem. Soc.*, **95**, 5508 (1973).
(23) "American Petroleum Institute Selected UV Spectral Data, Vol. 1, Ser. 130, Thermodynamic Research Center, Texas A&M University, 1970.
(24) U. B. Birks, "Photophysics of Aromatic Molecules", Wiley, New York, N.Y., 1970.
(25) C. A. Parker, "Photoluminescence of Solutions", Elsevier, Amsterdam, 1968.
(26) F. Wilkinson in "Fluorescence Theory, Instrumentation and Practice", G. G. Guilbault, Ed., Marcel Dekker, New York, N.Y., 1967.
(27) M. Gratzel and J. K. Thomas, *J. Am. Chem. Soc.*, **95**, 6885 (1973).
(28) F. Wilkinson and J. T. Dubois, *J. Chem. Phys.*, **39**, 377 (1962).
(29) P. Mukerjee, *J. Phys. Chem.*, **66**, 943 (1962).

Electrochemiluminescence from the Thianthrene–2,5-Diphenyl-1,3,4-oxadiazole System. Evidence for Light Production by the T Route

Paul R. Michael and Larry R. Faulkner*

Contribution from the Department of Chemistry, University of Illinois, Urbana, Illinois 61801. *Received March 24, 1977*

Abstract: The chemiluminescent reaction between the thianthrene (TH) cation radical and the anion radical of 2,5-diphenyl-1,3,4-oxadiazole (PPD) has been studied by the triple step technique. Emission transients decay very quickly and their magnitudes are extremely sensitive to the surface condition of the electrode. The current during the second step adheres very closely to that predicted by digital simulation, and this agreement is taken as evidence that the diffusion patterns in solution are accurately modeled by the simulation. The light intensity is proportional to the square of the redox reaction rate. This observation is incompatible with the generation of any significant component of luminescence by the S route. It does correspond to a limiting case of pure T-route behavior. A new type of experiment, in which the electrode is pulsed back to the initial potential for a brief interval during the second step, has demonstrated unequivocally that the chemiluminescence arises after a few milliseconds from a solution phase reaction zone, rather than from the electrode surface. Absolute light measurements give an emission efficiency, ϕ_{ecl}, on the order of 10^{-4}. The precise value is highly dependent on conditions.

The electron transfer reaction between the radical cation of thianthrene (TH) and the radical anion of 2,5-diphenyl-1,3,4-oxadiazole (PPD) yields light mainly from the first excited singlet state of thianthrene, $^1TH^*$.[1] Keszthelyi, Tachikawa, and Bard showed early that this system follows the pattern of behavior that is generally associated with the so-called S route to chemiluminescence,[1-3] in which the emitting singlet is populated directly in the redox event itself.

$$TH^+ + PPD^- \rightarrow {}^1TH^* + PPD \quad (1)$$

$$^1TH^* \rightarrow TH + h\nu \quad (2)$$

That is, the redox process is energetic enough to populate $^1TH^*$ (see Table I), and there is no magnetic effect on the chemiluminescence.

Magnetic effects have been used frequently as a diagnostic tool for the differentiation of mechanisms for redox chemiluminescence.[1-7] Enhancements of emission with increasing field strength have been observed for every studied case of energy-deficient luminescence (i.e., one involving a redox reaction that

is energetically unable to populate to observed emitting singlet). Light from such systems is believed to arise usually by redox excitation to a triplet which then undergoes triplet–triplet annihilation (T route to emission). The magnetic effects have been ascribed to field-dependent rate constants for triplet–triplet annihilation[2,8,9] and for the quenching of triplets by radical ions.[2,4,7,10] In contrast, no significant magnetic effect has been seen in any approximately energy sufficient case, except the energetically marginal rubrene cation–anion reaction.[2,5-7] The consistency of these results has led to the widely accepted plausibilities that magnetic effects can be used reliably as an indicator of mechanism and that electrochemiluminescence (ecl) arises mainly by the S route, whenever that path is energetically possible. If TH–PPD is indeed an S-route system, then the light emission rate I (einsteins/s) is related to the electron transfer rate N (mol/s) by

$$I = \phi_f \phi_s N \tag{3}$$

where ϕ_s is probability of singlet formation in electron transfer and ϕ_f is the fluorescence efficiency of $^1TH^*$. Both ϕ_s and ϕ_f are constants of the experimental system; hence S-route behavior implies a rigid linear linkage between I and N.

We shall show below that I in the TH–PPD system is not proportional to N but instead to N^2. Such behavior is inconsistent with the S route or an ST mixture, and can be understood within existing mechanistic models only via a pure T route. The simplest such process is

$$TH^+ + PPD^- \rightarrow {}^3TH^* + PPD \tag{4}$$

$$^3TH^* + {}^3TH^* \rightarrow {}^1TH^* + TH \tag{5}$$

$$^1TH^* \rightarrow TH + h\nu \tag{6}$$

These results demonstrate that ideas about the interpretation and diagnostic utility of magnetic effects must be revised, and they also cast doubt on our current understanding of the effects of reaction energy on the mechanism for chemiluminescence.

Experimental Section

The basic tool of this investigation was the triple step technique, in which the two reactants are generated electrochemically from a quiescent acetonitrile solution containing TH and PPD.[2,3,11-14] The experiment begins with the planar microelectrode at a potential where no oxidation or reduction takes place. At $t = 0$, the potential is stepped to a value in a region for diffusion-controlled generation of the first reactant (either TH^+ or PPD^-). This forward step lasts for a period t_f, then the potential is changed to a value in the region for diffusion-controlled production of the second reactant. This second, or reversal, step also lasts for a period t_f, then the potential is shifted back to the initial value, where both reactants are electrolytically destroyed. Time measured into the second step from its start is denoted by t_r. The reactants diffuse together during the second and third steps and react with a monotonically decreasing rate N. Light appears as a pulse that decays away as N declines. The shape of the light decay $I(t_r)$, in comparison to $N(t_r)$, contains the mechanistic information of interest. Experiments like these were proposed initially by Feldberg, who provided early interpretive schemes.[11,12] Additions and improvements to his methods for treating data have been advanced by others.[13,14]

Chemicals. Thianthrene (TH) and 2,5-diphenyl-1,3,4-oxadiazole (PPD) were either used as received from Aldrich or recrystallized from benzene. Recrystallization produced no changes in their electrochemical or spectroscopic behavior.

Tetra-*n*-butylammonium fluoroborate ($TBABF_4$) or tetra-*n*-butylammonium perchlorate (TBAP) was used as the supporting electrolyte, always at a concentration of 0.100 ± 0.001 M. Either they were supplied by Southwestern Analytical Chemicals (Electrometric Grade) and recrystallized from 5:1 ethyl acetate–pentane according to House,[38] or they were synthesized from the corresponding acid and tetra-*n*-butylammonium hydroxide and purified by recrystallization from 2:1 methanol–water and 5:1 ethyl acetate–pentane. Finally, the electrolytes were dried at 90 °C in vacuo for at least 48 h and stored over P_2O_5. Each purified batch was required to show an absorbance in 0.1 M solution of less than 0.1 cm^{-1} in the 200–250-nm region and less than 0.01 cm^{-1} for wavelengths longer than 250 nm.

Table I. Electrochemical and Spectroscopic Data

Compd	Peak potentials, V vs. SCE[a]		Energy levels, eV	
	$E_p(R/R^{+\cdot})$	$E_p(R/R^{-\cdot})$	E_s	E_t
TH	1.25	Not reduced	3.0[b,c]	2.6[a]
PPD	Not oxidized	−2.17	3.9[c,d]	2.5[a]

[a] Taken from ref 1. [b] Estimated from data presented by E. A. Chandross and D. J. Freed, *J. Am. Chem. Soc.*, **97**, 1274 (1975). [c] Compare with the free energy of the redox process, $\Delta G° = -3.36$ eV. [d] I. B. Berlman, "Handbook of Fluorescence Spectra of Aromatic Molecules", Academic Press, New York, N.Y., 1965.

Spectroquality acetonitrile from Matheson Coleman and Bell was used as the solvent. It was purified further by passing it through an activated alumina column into an evacuated reservoir.[15] The alumina had been treated beforehand by heating at 400 °C for 48 h under a vacuum. From the reservoir, the solvent was transferred sequentially to two flasks containing fresh P_2O_5 by bulb-to-bulb distillation on a vacuum line. Finally, it was transferred into the ecl cell in the same manner. After passing through the alumina column, the solvent was not allowed to contact the atmosphere at any further stage of sample preparation.

Electrochemical Cell and Sample Preparation. The electrochemical cell has been described in detail elsewhere.[16] It was designed to fit into the photometric apparatus described previously, and it resembled that of Bezman.[13,17] The working electrode was a polished Pt disk having a geometric area of either 3.3 or 3.8 mm^2. The counter electrode was a 7-cm length of 30 gauge Pt wire coiled into a position outside the photometric viewing area. A second length of this wire served as quasi-reference electrode (QRE). A glass sheath controlled its access to the current path so that it sampled the potential very near the working electrode. The tip of the QRE was no further than 3 mm from the disk. For a solution of 0.1 M $TBABF_4$ in acetonitrile, the time constant for double layer charging was typically ~90 μs.

Solutions were prepared in an auxiliary apparatus that allowed collection and condensation of the purified solvent vapor, dissolution of the weighed solutes to create a solution having a volume of 25.0 ± 0.2 mL, degassing of the solution by at least three freeze–pump–thaw cycles, and finally transfer of the working solution into the evacuated cell itself. All of these operations were carried out without allowing contact with the atmosphere or stopcock grease. After filling, the cell was sealed by a Teflon needle valve, and the auxiliary apparatus was removed. The details of these procedures have been presented elsewhere.[16]

Instrumentation. A Data General Nova 820 minicomputer controlled both the electrochemical generation of radical ion reactants and the acquisition of the light decay data. The software for these operations has been described.[16]

The potentials used for production of the radical ions were enforced by a Princeton Applied Research Model 173 potentiostat equipped with a Model 176 I/E converter. The potentiostat's input was programmed by the computer, which operated through a 12-bit D/A converter. Measurements of charge passed through the cell could be accomplished by connecting the working electrode directly to a custom-built analog current integrator, whose output was monitored by the computer through a sample-and-hold amplifier and an 8-bit A/D converter.

The photomultiplier was part of the integrating-sphere detector described previously.[16,18] This detection system was calibrated for absolute light measurements as noted earlier.[16,18] Its output fed a separate I/E converter, which drove a voltage scaler constructed from fast operational amplifiers. The gain of the scaler was selected by the computer from the sequence 1, 2, 5, . . . , 200, and each gain was accurate to better than 1%. The scaler output was read by the computer through a sample-and-hold amplifier, whose output was converted by a 10-bit A/D converter. The time constant for photometric measurements was governed by the I/E converter. For the experiments described here, it was 0.7 ms.

Timing for all measurements was controlled by a 10-MHz crystal oscillator in the computer interface.

Fluorescence and ecl spectra were recorded on an Aminco-Bowman

spectrophotofluorometer (SPF) equipped with a Hamamatsu R446S photomultiplier. Factors for correcting emission spectra were obtained as described previously.[16,18] Spectra displayed here were recorded with 6-nm emission band-pass.

Experimental Procedure. Since the potential of the QRE on an absolute scale is subject to slow drift, the potentials to be used in each triple step experiment for the generation of radical ions were determined immediately beforehand by cyclic voltammetry. After the voltammogram was recorded, the solution was stirred briefly, then allowed to rest for 5 min before the step experiment began.

The experiment started with entry of the step potentials and the step duration, t_f, at the keyboard. The potential for generation of each ion was routinely set at a value 250 mV more extreme than the corresponding cyclic voltammetric peak potential in order to ensure rapid establishment of a diffusion-limited reaction at the working electrode. The initial potential was 0 V vs. QRE. An option was available to pulse the working electrode back to 0 V vs. QRE during the second step. The beginning point and the length of this zero pulse were both variable.

The output of the QRE was sampled at $t = 0$ and $t = t_f$ to determine the total charge passed through the cell in the forward step. At $t = t_f$, the generation of the second reactant was begun and the sampling of the light decay curve was initiated. The data were taken at regularly spaced intervals of $t_f/500$ for the remainder of the reversal step and for $0.5t_f$ thereafter. During the recording operation, the computer used the scaler to maintain the signal at the A/D converter at a value between 30 and 100% of full scale, if possible. In addition, it measured background signals at each scale setting and corrected the ecl intensities appropriately. Finally, the program converted each intensity to a floating point form and scaled all values to a common basis. The total light output was obtained by integrating the decay curve according to Simpson's rule.

Electrochemical current transients were recorded in a similar manner by substituting the potentiostat's I/E converter for the photometric current follower.

Results and Discussion

Electrochemistry. The uncomplicated electrochemistry of this ecl system has been described.[1] In our apparatus, TH was oxidized to the stable cation radical at 0.92 V vs. QRE, and PPD was reduced to the stable anion at −2.55 V vs. QRE.

For scan rates up to 100 mV/s the peak separation for TH oxidation was 60 mV, which signified reversible one-electron oxidation. Our highest scan rate, 500 m/s produced a peak separation of 75 mV, but this value can probably be partly attributed to uncompensated resistance. The ratio of the reverse and forward peak currents was determined by the method of Nicholson.[19] For the slowest sweep rate of 50 mV/s, $i_{pc}/i_{pa} = 1.01$. Thus, $TH^{+\cdot}$ was completely stable for the time domain of the experiment.

Double step chronocoulometry was also used to study the TH oxidation. Christie[20] has shown that in the absence of adsorption or complicating chemical reactions the charge (Q) passed during the experiment should follow the relationship

$$\left|\frac{Q(2\tau) - Q(\tau)}{Q(\tau)}\right| = 0.5858 \qquad (7)$$

where τ is the duration of the forward step. In these studies, as in the triple step experiments, the potential applied to the working electrode was set 250 mV beyond the cyclic peak potential. For step times ranging from 10 ms to 2 s, the above ratio yielded an average value of 0.59 with an average deviation of 0.04. This supports the previous evidence that the oxidation of TH is a simple reaction leading to a stable cation radical.

PPD exhibited some degree of charge transfer irreversibility, as manifested by a voltammetric peak separation greater than 60 mV. Data from a scan rate study allowed an evaluation of the standard heterogeneous rate constant ($k_{s,h}$) by the method of Nicholson.[21] Scan rates from 50 to 500 mV/s yielded $k_{s,h} = 1.4 \times 10^{-2}$ cm/s for electrodes prepared in our standard manner, which involved polishing to a mirror finish with 600 grit alundum powder. The data used in calculating $k_{s,h}$ were typical; however, different electrode preparation techniques may produce different values for $k_{s,h}$. The relatively sluggish electrode kinetics did not greatly affect the triple step experiments. With the application of 250 mV potential oversteps, the peak of the light decay curve was reached in less than 1 ms regardless of the radical ion generation sequence.

This degree of irreversibility meant that the stability of PPD^- could not be validly assessed by comparing the forward and reverse peak heights in the conventional manner. Double step chronocoulometric studies were conducted over the same time range as those for the TH case. The ratio defined in eq 7 was equal to 0.58 ± 0.02. Thus, the PPD radical anion is also produced in a chemically simple electrode reaction and is stable over the time domain of these experiments.

As a check for the possibility of adsorbed species, the double step chronocoulometric technique of Anson was used to study both the TH and PPD radical ion formation.[22] For 50-ms step times, the results indicated possible net adsorptions of the radical ions, but for both TH^+ and PPD^-, the charge required to remove any adsorbed species was 0.25 μC or less. Since the Faradaic charge passed in the forward step of an ecl experiment in which $t_f = 1$ s is on the order of 25 μC, adsorbed species contributing 1% of this charge probably would not have an appreciable effect on the ecl experiment.

Slopes of the Q vs. $t^{1/2}$ plots, together with the geometric electrode area, yielded average diffusion coefficients of 2.7×10^{-5} and 2.6×10^{-5} cm²/s for TH and PPD, respectively. These compare favorably with the results reported by Keszthelyi et al. of 2.9×10^{-5} cm²/s for TH and 2.8×10^{-5} cm²/s for PPD, as calculated from the cyclic voltammetric peak heights.[1]

Luminescence Spectra and Efficiencies. Figure 1a shows corrected spectra for ecl emission and thianthrene fluorescence. The ecl spectrum was recorded by scanning the SPF while the working electrode was alternated at a 10-Hz frequency between potential limits selected as described above for the triple step experiments. An essentially identical, but noisier, ecl spectrum was obtained point by point via individual triple step experiments in which the integrated emission at a discrete wavelength was recorded. The close resemblance between the spectra of ecl and thianthrene fluorescence is apparent. The shapes are identical on the short wavelength side, and this correspondence strongly suggests $^1TH^*$ as a primary emitter. However, the ecl spectrum shows an enhanced intensity in the long-wavelength region. Figure 1b is the net ecl emission after the normalized thianthrene fluorescence distribution has been subtracted. The origin of this light is uncertain.

Several possible explanations can be disqualified. The long-wavelength emission cannot be attributed to inner filter effects or medium effects, because the solutions do not absorb appreciably at wavelengths where $^1TH^*$ emits, and the TH fluorescence spectrum is insensitive to the presence of $TBABF_4$. Since the PPD fluorescence peak is near 350 nm,[1] emission from $^1PPD^*$ is certainly not responsible. Excimer emission is conceivable, but the observed emission is probably at too low an energy to be assigned to a PPD excimer, and studies in this laboratory with solutions of TH at saturation (~10 mM) in deaerated acetonitrile showed no spectral differences in fluorescence, as compared to more dilute solutions. Thus, it is not reasonable to assign the long-wavelength ecl to thianthrene excimers formed conventionally by

$$^1TH^* + TH \rightleftarrows {}^1TH_2^* \qquad (8)$$

The analogous heteromolecular process yielding the exciplex (PPD^-TH^+) can be eliminated as well, because 1.5 mM PPD has no effect on TH fluorescence. Given the chemical stability of the system, it is also unreasonable to suspect that the green component arises from radical ion decay products excited either directly in their own ecl reactions or by sensitization from

Table II. Ecl Efficiencies[a]

Forward step time, s	$\phi_{ecl} \times 10^4$ +/−[b]	$\phi_{ecl} \times 10^4$ −/+[c]
Before Electrode Pretreatment		
0.5	<0.05	0.69
1.0	<0.05	0.56
2.5	<0.05	0.50
After Electrode Pretreatment		
0.5	1.6	2.5
1.0	1.3	2.0
2.5	1.0	1.2

[a] 1 mM TH, 1 mM PPD, 0.1 M $TBABF_4$ in acetonitrile. [b] Anodic forward step. [c] Cathodic forward step.

^{1}TH*. Sufficient concentrations could not be produced without being detected.

Other explanations deserve further examination: (1) The emission could come from a TH-PPD exciplex produced in the radical ion reaction or in a mixed triplet-triplet annihilation.[23-25] (2) It could represent an excimer of thianthrene produced in triplet-triplet annihilation or in redox reactions involving ionic aggregates. (3) It may arise from triplet annihilation involving low level impurities sensitized by ^{3}PPD* or ^{3}TH*. (4) It could be phosphorescence from ^{3}PPD* or ^{3}TH*, both of which reportedly have energies near the peak in Figure 1b.[1,26]

Ionic association requires careful consideration because Szwarc and co-workers have actually observed the aggregation of thianthrene radical cations in propionitrile.[27] The radical cation is in its monomeric form at room temperature at 1×10^{-4} M and has a single peak at 543 nm in its visible absorption spectrum. At −80 °C and a concentration of 5×10^{-3} M, the presence of a thianthrenium perchlorate aggregate can be seen by a double banded absorption spectrum with peaks at 470 and 594 nm.

Because the formation of such a complex in our system might affect the ecl spectrum (e.g., by possibility (2) above) and complicate the analysis of emission transients, a study similar to that of Szwarc et al. was performed with acetonitrile solutions. The thianthrenium perchlorate was synthesized according to the method of Murata and Shine.[28] The acetonitrile was treated as described above. The solutions were prepared in a drybox and spectra were recorded on a Cary Model 14 spectrophotometer with a 1-mm absorption cell. At a concentration of 1 mM at room temperature, only a single absorption peak was observed near 540 nm. At 5×10^{-3} M in the presence of 0.1 M $TBABF_4$, a small increase in absorbance was noted in the 470-nm region relative to the peak at 540 nm. This evidence suggests that the aggregate may be present in the more concentrated solution, although to only a small degree. From the absorption data it was concluded that for the 1 mM concentrations used in the ecl experiments, formation of thianthrenium aggregates does not occur to a significant extent in acetonitrile at room temperature, especially not in the ecl reaction zone where radical concentrations are minimal.

Possibility (4), which involves phosphorescence from fluid solutions at room temperature, might seem very unlikely; however, we note that Bonnier and Jardon have reported phosphorescence from thianthrene at 25 °C in cyclohexane.[29] They found a high triplet yield (0.94) from intersystem crossing and a triplet lifetime of 172 μs. In addition, Park and Bard reported benzophenone phosphorescence from several ecl systems.[30] Thus, triplet emission remains a possibility as the source of the long-wavelength tail.

It is not possible to be much more specific about the origin of this tail. We can only add that the time dependence of emission from the tail appears to be the same as that of the shorter wavelength luminescence.

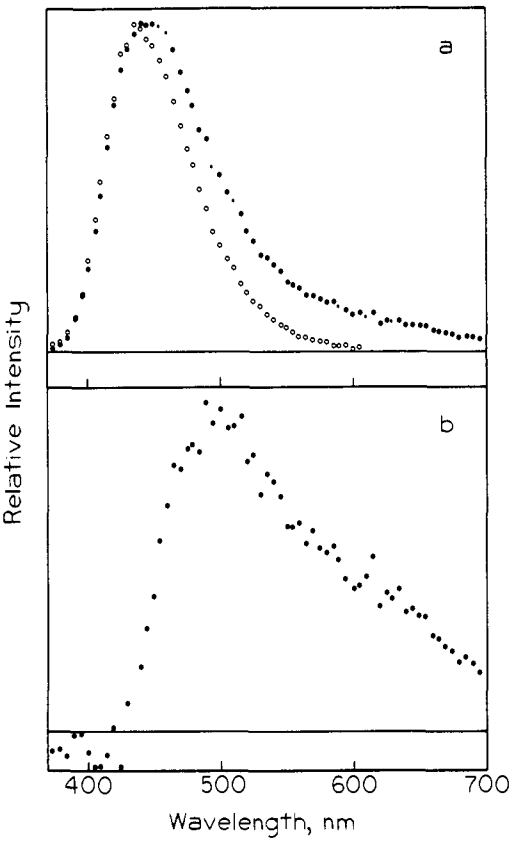

Figure 1. Corrected emission spectra from the TH-PPD system in acetonitrile: (a) ecl from 1 mM TH, 1 mM PPD, and 0.1 M $TBABF_4$ (filled circles) and fluorescence from 1 mM TH with right angle viewing (open circles); (b) ecl emission with TH fluorescence band subtracted.

The ecl emission efficiency was computed from total quantum output measurements as described in earlier publications.[13,16,18] The effective sensitivity of the photometric apparatus was calculated for the ecl spectrum of Figure 1a and was equal to 1.1×10^{13} photons/μC.[18] Correction for electrolytic destruction of reactants in the third step was made via the factor θ, which was applied as described previously.[13,31] Table II contains the efficiency data for the TH-PPD system. As indicated, sets of data were obtained before and after pretreatment of the working electrode. The pretreatment procedure consisted of holding the working electrode nominally at −5 V for 0.5 s in an unstirred solution. After a return to 0 V vs. QRE, a large (>10 μA) anodic current flowed through the cell. The electrode was maintained at 0 V and finally stirred for several minutes until the current had fallen to a negligible (<10 nA) value.

This pretreatment was found to increase permanently the light efficiency of the experiments involving initial generation of the radical cation by more than a factor of 20, while it roughly tripled emission from experiments using the opposite generation sequence. Other than the increase of light intensity, the only observable effect was a shift in the cyclic voltammetric peak potentials, which indicated some change in the condition of the QRE. Pretreatment did not produce any impurity peaks or change the background limits relative to the peak potentials.

It is important to realize that the intensity increase occurred after passing a charge of only 500 μC through the cell. This could produce an electrochemical product concentration of at most 2×10^{-7} M in 25 mL of solution. The final concentration may have been much less because of the anodic electrolysis at

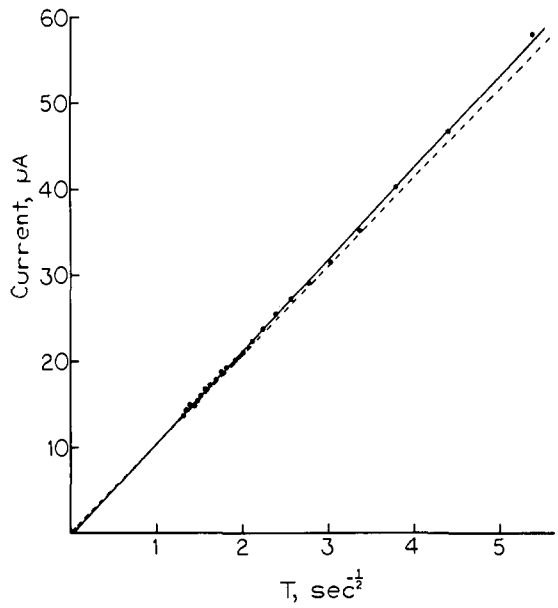

Figure 2. Comparison of measured (points and solid line) and predicted (dashed line) electrochemical currents. Conditions are detailed in the text.

0 V after the pretreatment. The 3-mm^2 electrode used in this experiment was clearly incapable of electrolyzing the entire bulk of the unstirred solution in 0.5 s. However, it could have produced some scavenger species that selectively removed triplet quenchers (see below) from the solution. Perhaps a more plausible explanation is that the −5 V pulse altered the surface condition of the electrode to impede the electrochemical production of quenchers from some trace impurity, e.g., oxygen from water.

From an inspection of ϕ_{ecl} in Table II, it is apparent that light production is a very inefficient process for this system. Only about one electron transfer event in 10 000 ultimately produces a photon. With the fluorescence efficiency of TH equal to 0.04,[29] one can add that approximately one electron transfer event in 400 produces ^{1}TH*. It will be possible to comment further about the efficiency of redox excitation after the data from the ecl decay curves have been discussed.

Decay Curves. The analysis of luminescence decay curves produced by triple step experiments is based on a comparison of the absolute light emission rate to the rate of the homogeneous electron transfer reaction as modeled by digital simulation. Before proceeding with a discussion of the light transients, it is first necessary to establish that the digital simulation can faithfully represent the concentration profiles and the diffusion of the reactants in the bulk solution. The experimental quantity that reflects them most clearly is the current decay during the second step.

One can show rigorously that the current transient follows the equation[32]

$$i = \frac{FAD^{1/2}C}{\pi^{1/2}}[2t_r^{-1/2} - (t_r + t_f)^{-1/2}] \qquad (9)$$

under the assumptions that the diffusion coefficients of all species are equal to D and the bulk concentrations of both ion precursors are C. For the experiments described below, these two assumptions are very nearly true.

Rearrangement of this equation to provide a dimensionless current parameter Z, suitable for comparison with conventional simulation output, yields

$$Z = \frac{it_f^{1/2}}{FAD^{1/2}C} = Tt_f^{1/2}/\pi^{1/2} \qquad (10)$$

where $T = 2t_r^{-1/2} - (t_r + t_f)^{-1/2}$. We note also that this relationship holds regardless of the rate constant for the radical ion annihilation.[11,16,32] This point is verified by the fact that simulations involving rate constants varying from zero to infinity all provide the same current transient, which adheres extremely closely to eq 9.

This linear linkage between the current and the parameter T provides the format for the comparison between real and predicted currents shown in Figure 2. The theoretical current for a given value of T was obtained by multiplying the corresponding simulated Z value by the factor $FACD^{1/2}/t_f^{1/2}$, which was evaluated directly from chronocoulometric data acquired during the forward step. The data points show measured currents taken from $t_r/t_f = 0.1$ to 1. They were obtained from an acetonitrile solution 1 mM in TH and PPD and 0.1 M in $TBABF_4$. The experiment was initiated by a cathodic step, and t_f was equal to 1 s. The least-squares slope of the data is within 4% of that of the dashed line showing the predictions of the simulation. Equivalent results were obtained for experiments in which the initial step was anodic. The small difference between the predicted and observed slopes can be attributed to inaccuracies in the assumption that the diffusion coefficients of the two parent compounds and their radical ions are all equal.

The close agreement in Figure 2 implies that the digital simulation accurately describes the diffusion processes during the ecl experiment, and this conclusion provides assurance about the simulation's ability to predict the time dependence of the total redox reaction rate, N. The simulation actually supplies N as the dimensionless parameter $\omega_n = Nt_f^{1/2}/AD^{1/2}C$, but for any given experiment, the time dependence of ω_n is the time dependence of N. Our simulations were based on diffusion-controlled radical ion annihilation, but Feldberg showed some time ago that ω_n is independent of the redox rate constant k as long as $k > 100/t_fC$.[11] Therefore, as long as k exceeds 10^5 M^{-1} s^{-1}—and it is believed to be several orders of magnitude greater—the simulated ω_n must be an accurate experimental reaction rate in our systems.

With ω_n in hand, one can proceed to an analysis of the actual light transients. The goal of this kind of study is to uncover the linkage between the reaction rate N and the total absolute absolute emission rate I, or, equivalently, between their dimensionless representations ω_n and $\omega_i = It_f^{1/2}/AD^{1/2}C$. Initial work was done with the curve fitting algorithm developed earlier.[14] The low-intensity luminescence decayed away quickly, so that during the time period used for Feldberg plots ($\log \omega_i$ vs. $(t_r/t_f)^{1/2}$ in the range of $t_r/t_f = 0.2$–1)[12,13] the data were too noisy to obtain reliable slopes and intercepts. An advantage of the curve fitting technique is that it uses the early time region of the decay curve where the signal to noise ratio is high.

The original fitting program was designed for application only to triple step ecl experiments in which both reactants were derived from a single parent, and ω_n was calculated from an approximate analytical form. Because this approach would not be applicable to mixed ecl systems or to some of the potential programs that were to be applied, the fitting routine was modified to accept any set of ω_n's. The sets supplied to the fitting routine were actually composites generated from three simulations. The time intervals $0 < t_r/t_f \leq 0.01$, $0.01 < t_r/t_f \leq 0.1$, $0.1 < t_r/t_f \leq 1$ were modeled separately in simulations having resolutions of 10^5, 10^4, and 10^3 iterations per step, respectively, so that each time segment could be treated with adequate resolution.[14] In each simulation the dimensionless homogeneous redox rate constant kt_fC was set equal to the number of iterations per step to provide a smooth ω_n set for the curve fitting program. Experimentally, this was indistinguishable from using an infinite rate constant.[14]

The fitting algorithm is based on the proposed general

Table III. Decay Curve Parameters[a]

Pretreatment[b]	Zero pulse[c]	$\alpha \times 10^2$	β	γ	$(\alpha^2/\beta) \times 10^4$
		Cathodic Forward Step			
No	No	6.72	15.1	1.26×10^{-9}	2.99
No	Yes	9.23	25.6	1.11×10^{-7}	3.33
Yes	No	2.79	1.07	2.49×10^{-5}	7.27
Yes	Yes	9.37	12.6	2.42×10^{-5}	6.97
		Anodic Forward Step			
No	No	6.04	15.9	3.72×10^{-9}	2.29
No	Yes	6.09	15.3	1.74×10^{-9}	2.42
Yes	No	2.78	1.70	1.81×10^{-5}	4.55
Yes	Yes	6.82	11.2	3.18×10^{-5}	4.15

[a] 1 mM TH, 1 mM PPD, 0.1 M $TBABF_4$ in acetonitrile. $t_f = 0.5$ s. [b] See text for description of pretreatment procedure. [c] Zero pulse applied from $t_r = 50$ to 60 ms.

equation linking ω_i to ω_n for an ST system:

$$\omega_i = \beta - (\beta^2 + \alpha\beta\omega_n)^{1/2} + 0.5\,\alpha\omega_n + \gamma\omega_n \qquad (11)$$

The parameters α and β are aggregates of kinetic variables relating to the T path, whereas γ is the chemiluminescence efficiency of the S route.[14]

Results of the three-parameter fit for the TH–PPD decay curves are listed in Table III. One feature that is common to each of the eight experimental conditions is the small γ. When γ becomes insignificant the precision in determining it becomes poor, as indicated by its large fluctuation. The physical meaning of this result is that there is no discernible component of emission which is directly proportional to ω_n; thus the fraction of S-route emission is negligibly small or zero for t_r greater than 5 ms. This point is amplified by more detailed examination of the decay curves.

Since γ is negligible, we can rewrite eq 11 as

$$\omega_i/\beta = 1 - (1 + \alpha\omega_n/\beta)^{1/2} + 0.5\alpha\omega_n/\beta \qquad (12)$$

For the ratios of α/β in Table III, the expression $\alpha\omega_n/\beta$ is always much less than unity over the fitting interval. This allows the square root term in eq 12 to be evaluated conveniently by a Maclaurin series. Using the first three terms of the series and simplifying, one obtains the limiting case,[12]

$$\omega_i = \alpha^2\omega_n^2/8\beta \qquad (13)$$

Equation 13 shows that the data at hand allow neither α nor β to be evaluated individually. The quantity $\alpha^2/8\beta$ is simply the proportionality constant between ω_i and ω_n^2, and it should be a true constant for a given experiment. This prediction was verified by supplying the curve fitting program with different starting values of α, β, and γ in separate trials with a single experimental decay curve. The final values of α and β varied over an order of magnitude, but α^2/β was constant to within less than 1%.

The fast decay of luminescence was unexpected and prompted concern that the light might arise from a surface reaction rather than the conventionally conceived homogeneous process. To test this possibility, we conducted a new type of experiment in which the working electrode was pulsed to 0 V vs. QRE for 10 ms during the second step. During the zero pulse, both reactant ions are electrolytically destroyed with regeneration of their parents. If light production occurs at the surface, the luminescence should immediately terminate upon application of the zero pulse and resume coincidentally with the end of the pulse. On the other hand, a homogeneous reaction taking place in a zone some distance from the electrode will feel effects from the changed boundary conditions at the surface rather slowly, because the effects are transmitted by diffusion.[33]

The results of an experiment in which the zero pulse was applied from $t_r/t_f = 0.10$ to 0.12 for $t_f = 0.5$ s are shown in Figure 3. Several conclusions can be drawn from the shape of the curve and the ability of the fitted simulation to model the data. The fact that the effect of the zero pulse on the light decay curve lagged the actual application of the zero pulse by almost 10 ms demonstrates that chemiluminescence arises from reactions in solution at a site far from the electrode, except at the earliest times in the second step. The simulation is again supported as an accurate model for the effect of the homogeneous redox reaction because it correctly predicts the time of the minimum at about $t_r/t_f = 0.13$. The ability of the fitting routine to handle this type of experiment and the agreement of $\alpha^2/\beta = 3.21 \times 10^{-4}$ with more conventional potential programs also support the argument that the information derived from the light decay curve is characteristic of the homogeneous reaction, at least for t_r greater than a few milliseconds. We emphasize that the fit shown in Figure 3, despite its apparent complexity, is really a one-parameter fit; the aggregate $\alpha^2/8\beta$ is the scale factor between ω_i and ω_n^2.

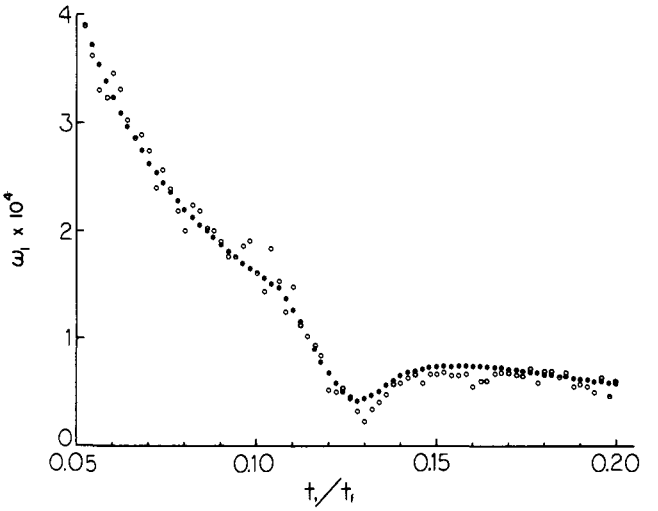

Figure 3. Comparison of the measured intensity (open circles) and the fitted simulation (closed circles) for the zero pulse experiment.

A more obvious demonstration of this point is made in Figure 4, which shows a plot of ω_i vs. ω_n^2. The linear relationship predicted by eq 13 is clearly borne out in the plot. The points represent every data point taken over the interval from $t_r/t_f = 0.02$ to 0.1 for an experiment in which the forward step was cathodic and $t_f = 0.5$ s. The least-squares slope of the line in Figure 4 is equal to 3.63×10^{-5} and agrees very well with $\alpha^2/8\beta = 3.74 \times 10^{-5}$ as determined by the curve fitting program.

An inspection of Table III reveals that α^2/β is relatively

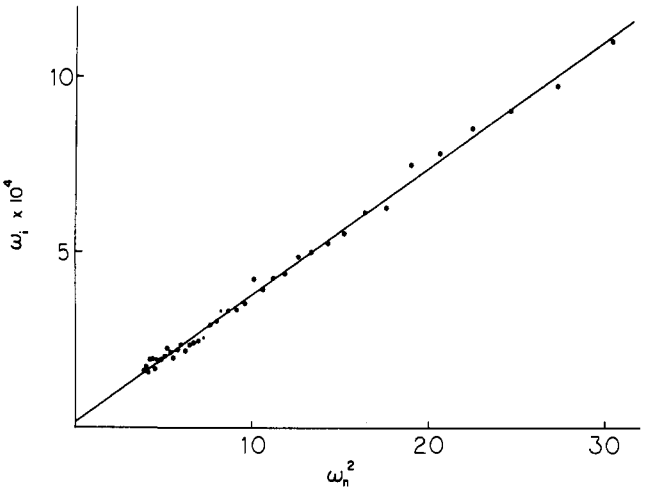

Figure 4. Plot illustrating the proportionality of ω_i to ω_n^2. Data correspond to the experiment described in the first line of Table III.

constant for a given working electrode condition and forward step direction. It ought to be independent of the application of a zero pulse because the ratio is characteristic of the solution phase reaction mechanism and not of the potential program. However, α^2/β is seen to depend on the direction of the initial step and the electrode pretreatment. This can be attributed to the sensitivity of the quenching term, β, to the presence of small, variable quantities of electrochemically influenced triplet quenchers.

Equation 3 shows that the S route cannot give a nonlinear relationship between I and N (or ω_i and ω_n) unless ϕ_f or ϕ_s, or both, depend on ω_n. Since the fluorescence lifetime of thianthrene is only about 30 ns,[29] it is totally unreasonable to postulate variations in ϕ_f in this system caused by time-dependent quencher concentrations. The necessary concentrations simply could not be achieved. Moreover, ϕ_s, which is a branching ratio for an elementary, solution-phase reaction, cannot show any time dependence. One could conceive of ϕ_f as rising with ω_n if stimulated emission played a role; however, the spectral shape shows no indication of such effects. Thus we conclude that the results are inconsistent with the production of light via the S route, as that route is now understood. On the other hand, the linear relationship between ω_i and ω_n^2, the low chemiluminescence yield, and the sensitivity of the system to the pretreatment procedure are easily understood in terms of the pure T route.

If the T route is assumed, one can comment on the efficiency ϕ_t with which triplets are populated in the redox process. From the measurement of ϕ_{ecl} we concluded that about 400 electron transfer events were required to produce one $^1TH^*$. The excited singlet yield of triplet–triplet annihilation is usually only on the order of a few percent. For a typical value of 0.05, one would find 20 electron transfers per triplet annihilation event. Since triplets are readily quenched by radical ions and other species, and since ω_i becomes proportional to ω_n^2 only when triplet–triplet annihilation is quite uncompetitive with pseudo-first-order triplet decay, the large majority of the triplets could not participate, then almost every electron transfer event would have to yield a molecule in its lowest triplet state. While ϕ_t is probably less than unity, previous experiments involving triplet interception techniques have shown values as high as 0.8 for the fluoranthene–10-phenylphenothiazine ecl system.[34] Even though the overall luminescent efficiency for the TH–PPD system is low, the excited state yield of the electron transfer reaction may be quite high. The inefficiency may arise from reactions following initial excited state production.[35]

The assignment of a pure T-route mechanism to this system certainly does not accord with the S-route mechanism implicated by studies of magnetic effects. Although this is a key point of disagreement, it may not reflect a fundamental conflict over the interpretation of the magnetic enhancements usually observed with T-route systems, because special conditions can cancel the field effect. Tachikawa and Bard found in delayed fluorescence experiments that, by carefully adjusting the concentration of a paramagnetic quencher concentration, the magnetic enhancement of triplet lifetime could exactly counteract the magnetic inhibition of triplet–triplet annihilation.[36] With reference to ecl, however, it seems unlikely that the paramagnetic quenchers in the reaction zone would be precisely at the right concentration to cancel the magnetic effect in every experiment. Moreover, the lack of a field effect in the TH–PPD system fits into the pattern of behavior generally observed for energy-sufficient systems.

The difference between the conclusions drawn from decay curve analysis and from magnetic effects might also be reconciled by considering the fact that the two experiments deal with different segments of the light pulse. The magnetic experiments were conducted by observing the effect of the field only on the height of the pulse.[1] No attempt was made to study the shape of the curve or its integral as a function of field strength. Decay curve analysis deals only with light emitted later than $t_r/t_f > 0.01$. It is conceivable that there is a dual mechanism in which light in the earliest part of the pulse arises via a field-independent S-route path, perhaps taking place only near the electrode surface in a special environment, while the redox reaction in solution yields only triplets producing the observed decay curves. However, the known ability of metal surfaces to quench excited singlets[37] could complicate this idea.

Acknowledgment. We are grateful to the National Science Foundation for its generous support of this work through Grant MPS-75-05361.

References and Notes

(1) C. P. Keszthelyi, H. Tachikawa, and A. J. Bard, *J. Am. Chem. Soc.*, **94**, 1522 (1972).
(2) L. R. Faulkner, *MTP Int. Rev. Sci.: Phys. Chem., Ser. Two*, **9**, 213 (1976), and references cited therein.
(3) L. R. Faulkner and A. J. Bard, *Electroanal. Chem.*, 7, 1 (1977), and references cited therein.
(4) L. R. Faulkner, H. Tachikawa, and A. J. Bard, *J. Am. Chem. Soc.*, **94**, 691 (1972).
(5) H. Tachikawa and A. J. Bard, *Chem. Phys. Lett.*, **26**, 246 (1974).
(6) N. Periasamy and K. S. V. Santhanam, *Proc. Indian Acad. Sci., Sect. A*, **80**, 194 (1974).
(7) H. Tachikawa, Ph.D. Dissertation, University of Texas at Austin, 1973.
(8) R. E. Merrifield, *J. Chem. Phys.*, **48**, 4318 (1968).
(9) (a) C. E. Swenberg and N. E. Geacintov in "Organic Molecular Photophysics", Vol. 1, J. B. Birks, Ed., Wiley, New York, N.Y., 1973; (b) *ibid.*, Vol. 2, 1974; and references cited therein.
(10) P. W. Atkins and G. T. Evans, *Mol. Phys.*, **29**, 921 (1975).
(11) S. W. Feldberg, *J. Am. Chem. Soc.*, **88**, 390 (1966).
(12) S. W. Feldberg, *J. Phys. Chem.*, **70**, 3928 (1966).
(13) R. Bezman and L. R. Faulkner, *J. Am. Chem. Soc.*, **94**, 3699 (1972).
(14) L. R. Faulkner, *J. Electrochem. Soc.*, **122**, 1190 (1975).
(15) T. Osa and T. Kuwana, *J. Electroanal. Chem.*, **22**, 389 (1969).
(16) P. R. Michael, Ph.D. Thesis, University of Illinois at Urbana-Champaign, 1976.
(17) R. Bezman and L. R. Faulkner, *J. Am. Chem. Soc.*, **94**, 6317 (1972); **95**, 3083 (1973).
(18) P. R. Michael and L. R. Faulkner, *Anal. Chem.*, **48**, 1188 (1976).
(19) R. S. Nicholson, *Anal. Chem.*, **38**, 1406 (1966).
(20) J. H. Christie, *J. Electroanal. Chem.*, **13**, 79 (1967).
(21) R. S. Nicholson, *Anal. Chem.*, **37**, 1351 (1965).
(22) F. C. Anson, *Anal. Chem.*, **38**, 54 (1966).
(23) K. A. Zachariasse, Thesis, Vrije Universiteit te Amsterdam, 1972.
(24) A. Weller and K. Zachariasse, *Chem. Phys. Lett.*, **10**, 590 (1971).
(25) S. M. Park and A. J. Bard, *J. Am. Chem. Soc.*, **97**, 2978 (1975).
(26) H. V. Drushel and A. L. Sommers, *Anal. Chem.*, **38**, 10 (1966).
(27) M. de Sorgo, B. Wasserman, and M. Szwarc, *J. Phys. Chem.*, **76**, 3468 (1972).
(28) Y. Murata and H. J. Shine, *J. Org. Chem.*, **34**, 3368 (1969).
(29) J. M. Bonnier and R. Jardon, *J. Chim. Phys. Phys.-Chim. Biol.*, **68**, 428 (1971).
(30) S. M. Park and A. J. Bard, *Chem. Phys. Lett.*, **38**, 257 (1976).

(31) R. Bezman and L. R. Faulkner, *J. Am. Chem. Soc.*, **94**, 6331 (1972); **95**, 3083 (1973).
(32) L. R. Faulkner, *J. Electrochem. Soc.*, in press.
(33) R. P. Van Duyne and S. F. Fischer, *Chem. Phys.*, **5**, 183 (1974).
(34) D. J. Freed and L. R. Faulkner, *J. Am. Chem. Soc.*, **94**, 4790 (1972).
(35) Note that the low overall efficiency of the T route probably eliminates the hypothesis that redox reactions proceed through $^1TH^*$, but the triplet pathway is fed efficiently by the high triplet yield via intersystem crossing. Even with ϕ_f as low as 4%, the S pathway should dominate any T-route emission arising in such a manner, if singlets are formed to any significant degree in the radical annihilation.
(36) H. Tachikawa and A. J. Bard, *Chem. Phys. Lett.*, **26**, 10 (1974).
(37) H. Bücher, K. H. Drexhage, M. Fleck, H. Kuhn, D. Möbius, F. P. Schäfer, J. Sondermann, W. Sperling, P. Tillmann, and J. Wiegand, *Mol. Cryst.*, **2**, 199 (1967).
(38) H. O. House, E. Feng, and N. P. Peet, *J. Org. Chem.*, **36**, 2371 (1971).

Detection of Proton Acceptor Sites of Hydrogen Bonding between Nucleic Acid Bases by the Use of ^{13}C Magnetic Resonance

Hideo Iwahashi and Yoshimasa Kyogoku*

Contribution from the Institute for Protein Research, Osaka University, Suita, Osaka, 565, Japan. *Received November 12, 1976*

Abstract: ^{13}C magnetic resonance spectra of 1-cyclohexyl derivatives of uracil, thymine, 5,6-dihydrouracil, 5-bromouracil, and 4-thiouracil and their 1:1 mixture with 9-ethyladenine were observed in chloroform solutions. The signals of the 2- and 4-carbonyl carbons show remarkable downfield shifts at higher concentrations. By computer analysis of the chemical shift–concentration curves, association constants and limiting shifts were obtained. From the values of the limiting shifts it can be inferred that the self-association using the 4-carbonyl group is more common in uracil and the ratio of the 4-carbonyl dimer to the 2-carbonyl dimer gradually falls in the order thymine, 5,6-dihydrouracil, 5-bromouracil, 4-thiouracil while that of the 2-carbonyl dimer rises in the order. However, with adenine association the ratio is highest in thymine and this is followed by uracil, 5-bromouracil, and 4-thiouracil in descending order of magnitude.

In the double-stranded structures of deoxyribonucleic acid and ribonucleic acid, adenine forms specific hydrogen bonds with thymine (or uracil) and guanine with cytosine. The specific bonds are believed to be the molecular basis of information transfer in nucleic acids. Much work has been done to find the basis of this specificity by the use of synthetic poly- and oligonucleotides and single base derivatives. Some infrared[1-8] and proton magnetic resonance studies[9-11] clearly showed that even single base residues interact by means of specific hydrogen bonds in solution. The data obtained in these experiments revealed the strength of interaction on the amino and imino protons, but little is known about the acceptor sites of the hydrogen bonds. In the base pair model proposed by Watson and Crick, thymine (or uracil) pairs with adenine by using the C-4 carbonyl group. However, x-ray analyses showed that 5-bromouracil[12] and 4-thiouracil[13] derivatives formed complexes with themselves and with adenine derivatives through the C-2 carbonyl group.

In the present experiment we observed ^{13}C magnetic resonances of single base derivatives in solution and tried to find interaction sites from the concentration dependency of chemical shifts. When hydrogen bonds are formed, ^{13}C nuclei at the nearer hydrogen bonded sites suffer perturbation in the electron distribution of the sites; this perturbation disturbs the diamagnetic circulation of electrons. The resultant downfield shift of the ^{13}C magnetic resonance is smaller than that of the ^1H resonance of the bonded proton, because the carbon atom does not participate directly in the hydrogen bonding and is located at least one bond from the site. Also the resonance frequency of ^{13}C is one-fourth that of ^1H. In spite of the smaller shifts, ^{13}C resonances promise to provide powerful information on the effect of the bonding on the molecule skeleton. The present experiment indicates the population of the carbonyl carbons bonded to hydrogen atoms and the population's dependency on substitution at the 5 position of the uracil residue.

Experimental Section

Materials. 9-Ethyladenine (A), 1-cyclohexyluracil (U), 1-cyclohexylthymine (TH), 1-cyclohexyl-5-bromouracil (BU), 1-cyclohexyl-5,6-dihydrouracil (DU), and 1-cyclohexyl-4-thiouracil (TU) were purchased from Cyclo Chemical Co., Los Angeles, Calif. 9-Ethyladenine was recrystallized from a mixture solvent of carbon tetrachloride and chloroform, and the other compounds were used without further purification. ^{13}C magnetic resonance spectra were measured for their chloroform-d_1 solutions. Chloroform-d_1 obtained from CEA, France, was dried by passing through an alumina gel column in a drybox. Chloroform is a favorable solvent for investigating intermolecular interaction because it has relatively weak polarity and scarcely interacts with adenine and uracil derivatives.

Methods. ^{13}C magnetic resonance spectra were obtained at 25 MHz with a JEOL PFT-100 pulse Fourier transform NMR system locked on deuterium. The protons were completely decoupled at 100 MHz for ^{13}C NMR spectra of all the uracil derivatives. Tetramethylsilane was used as an internal standard and chemical shifts were measured relative to the ^{13}C resonance of Me_4Si by data reduction. The spectrum of each uracil derivative was obtained in a concentration range from 0.2 to 0.025 M, and the spectra of mixtures with A were measured for solutions from 0.2 to 0.025 M. The temperature of the sample tubes was kept at 27 °C throughout the experiments.

Procedures for the Calculation of Association Constants and Population Differences. The equilibrium equation for the formation of a 1:1 complex of adenine and uracil derivatives is expressed as

$$A + U \rightleftharpoons AU \tag{1}$$

but in the present case, various conformations of dimers as shown in Figure 1 should be taken into account, because A and U have two proton acceptor sites each. Taking all the possibilities into account, the above relation can be rewritten as follows:

$$A + U \rightleftharpoons kA_1U_2 + lA_7U_2 + mA_1U_4 + nA_7U_4 \tag{2}$$

Here the relation of $k + l + m + n = 1$ holds for k, l, m, and n. Then the association constant K can be defined as follows:

$$K = C^k{}_{A1U2}C^l{}_{A7U2}C^m{}_{A1U4}C^n{}_{A7U4}/C_AC_U \tag{3}$$